



More Unintended Spurious Forces in Seismic Response History Analysis

Theodore L. Chang¹ and Chin-Long Lee^{2*}

¹Research Associate, IRIS Adlershof, Humboldt-Universität zu Berlin, Berlin, Germany, 12489

²Associate Professor, Department of Civil and Natural Resources Engineering, University of Canterbury, Christchurch 8041, New Zealand

*chin-long.lee@canterbury.ac.nz (Corresponding Author)

ABSTRACT

It has been well-known that incorrect use of damping models could result in spurious damping forces during seismic response history analysis of large-scale structures. There are, however, more sources that could also result in unintended spurious forces, not only for the damping force component but also for the constitutive member force and inertial force components. One of these sources is the incorrect interpolation or interpretation of the digitized seismic input motions. Recorded seismic ground motions are typically digitized with a time step between 0.005 and 0.02 sec. However, a structural model could have most of its structural periods way shorter than 0.005 sec, particularly due to unavoidable stiff elements and unintended parasitic modes. For accurate response, analysts would, therefore, choose a time step size for the response history analysis much smaller than the time step size used in the recorded input ground motions. It has been a custom in most analysis software that linear interpolation is used to obtain the ground motion data not sampled at the numerical analysis time steps. This conventional practice, unfortunately, would result in unintended spurious forces. In this paper, the spurious forces due to the linear interpolation of input ground motion data will be discussed with examples. Recommendations to avoid this consequence will also be presented.

Keywords: Spurious structural response, time stepping method, linear interpolation, filtering

INTRODUCTION

In the simulation of seismic response of structures, since the work of Chrisp [1], it has been well-known that unintended spurious damping forces may exist and affect the accuracy of structural responses. These spurious damping forces are due to an incorrect choice of viscous damping models based on the damping coefficient matrix for simulating un-modelled energy dissipation not yet incorporated using material hysteretic models. This problem has been studied in detail by many researchers [2-7]. Many solutions, as discussed by Lee [8], have been proposed. Unfortunately, there are other sources of spurious forces, such as errors due to collected input loads and spurious roots in pseudodynamic testing [9-10].

One of the sources of spurious forces is the improper interpretation of the recorded earthquake ground motions. Most recorded seismic ground motions are usually digitised with a time step ranging between 0.005 and 0.02 sec (the corresponding sampling frequency is 200 and 50 Hz, respectively), where a smaller time step is typically used for newer events due to advancement in the technologies of seismometers. Based on the Nyquist theorem [11], the components of the recorded ground motions can only be reliably recovered for frequencies of not more than the Nyquist frequency, which is half of the sampling frequency. In other words, for a sampling frequency of 50 Hz, or a sampling time step of 0.02 sec, the components of the recorded ground motions can only be reliably recovered for frequencies of at most 25 Hz. The components with frequencies beyond the Nyquist frequency are considered lost. When this digitized data is used as the input ground motion for analyzing the seismic response histories of a structure, the responses can only have their reliable components with frequencies up to 25 Hz.

This threshold of maximum frequency is, unfortunately, too restrictive for analyzing a typical civil structure or a multi-story building in a response history analysis. Most structures of interest have a wide range of natural frequencies. Although their first mode frequencies could be between 0.1 Hz and 10 Hz, their higher mode frequencies could be way above the Nyquist frequency of the recorded ground motions. These high-frequency components are usually due to unavoidable small and stiff elements in the analyzed structure, particularly when mesh refinement is used to improve the accuracy of responses. They have

significant effects on the structural responses, for example, inter-storey drifts, inter-storey shear forces, and floor accelerations. These responses are dominated by higher modes and would require a very small time step for good accuracy. It is, therefore, necessary in the response history analysis to have its analysis time step much smaller than the time step used in the recorded ground motions.

In a typical practice of structural analysis software, e.g. Abaqus [12] and OpenSees [13], the ground motion data not sampled at the analysis time step would usually be linear interpolated from nearby recorded data. As shown in a later section, this practice of linear interpolation essentially introduces into the ground motion spurious components of frequencies beyond the original Nyquist frequency. These spurious components would likely trigger the higher modes of the structure, thereby introducing spurious forces into the dynamic structural system and affecting the accuracy of structural responses.

This source of unintended spurious forces due to the linear interpolation of ground motion data is, however, rarely studied. This paper discusses this source of spurious forces and its effects on damping, inertial and constitutive member forces in the system. A response history analysis example will be conducted to showcase the effects. The following will first discuss the theory of linear interpolation and later provide recommendations on circumventing these spurious forces.

THEORY

Solution of SDOF System

Consider a single degree of freedom damped linear system. The equation of motion is often expressed as

$$ma(t) + cv(t) + ku(t) = p(t) \quad (1)$$

where m is the mass, c is the damping coefficient, k is the stiffness, a , v , u are time-dependent acceleration, velocity, and displacement, respectively, and p is the external load. It is possible to obtain the analytical solution to the above equation by using Duhamel's integral, which can be expressed in the frequency domain as follows

$$U(\omega) = H(\omega) \cdot P(\omega) \quad (2)$$

where $U(\omega)$ is the displacement function, $P(\omega)$ is the external load function that depends on the specific form of external load and can be computed via the Fourier transform, $H(\omega)$ is the transfer function that can be determined by the properties of the system, all expressed in terms of frequency ω .

By differentiation, one can further obtain the analytical solutions of velocity and acceleration, which can be used to compute force responses, as shown below

$$P_d(\omega) = c \cdot V(\omega) = c \cdot i\omega \cdot U(\omega) = c \cdot i\omega \cdot H(\omega) \cdot P(\omega) \quad (3)$$

$$P_i(\omega) = m \cdot A(\omega) = -m \cdot \omega^2 \cdot U(\omega) = -m \cdot \omega^2 \cdot H(\omega) \cdot P(\omega) \quad (4)$$

where $P_d(\omega)$ denotes the damping force response, $P_i(\omega)$ denotes the inertial force response, and i is the imaginary unit.

The above equations establish the relationship between external load and damping force and between external load and inertial force. Given that the transfer function H does not change with the external load, for a given linear elastic system, once P is known, P_d and P_i can be determined.

Linear Interpolation

For a response history analysis, for more accurate numerical results and better convergence performance in the case of inelastic analyses, a small time step size would typically be employed for time marching. This time step size is often smaller than that of the ground motion, which is typically sampled at a frequency between 50 Hz and 200 Hz. Thus, to perform time marching, linear interpolation would be used.

The original ground motion does not contain any components beyond its sampling frequency f_s . The components with frequencies between $f_s/2$ and f_s are unreliable and subject to aliasing. Linear interpolation effectively upsamples the original ground motion with a higher sampling frequency. Denoting the upsampling ratio by L , the actual ground motion used in a response history analysis is sampled at a rate of Lf_s . Such a procedure fills the additional frequency region from $f_s/2$ to $Lf_s/2$ with non-trivial components, which bear a risk of introducing spurious responses in the results.

Consider a sinusoidal wave,

$$f(t) = \sin(2\pi f_0 t) \quad (2)$$

where f_0 is chosen to be 25 Hz, that is, a period of 0.04 sec. Suppose it is sampled at a rate of 200 Hz. It can be plotted in both the time and frequency domains via a discrete Fourier transform (DFT). Figure 1 shows the time domain record up to 0.2 sec and the frequency domain component up to the Nyquist frequency.

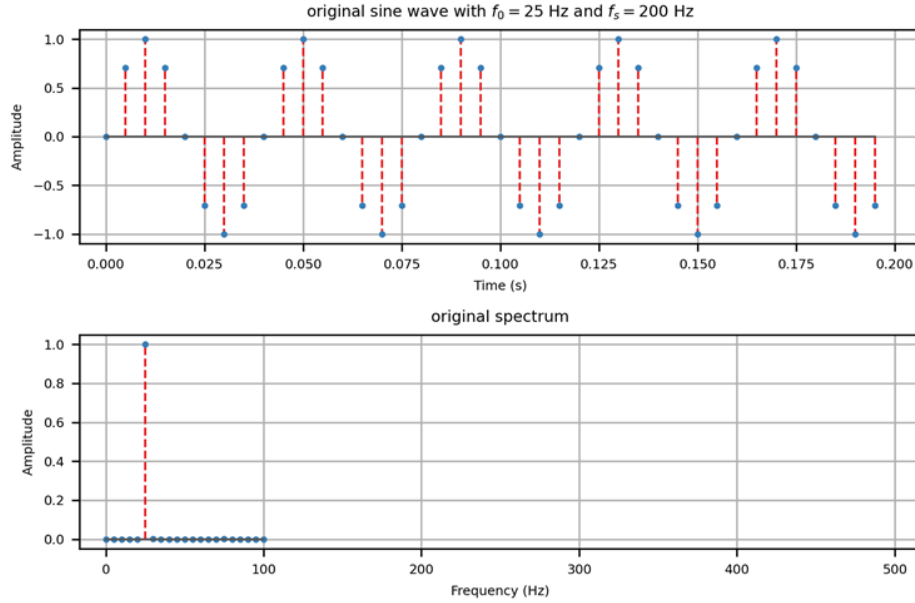


Figure 1. Time domain record and frequency domain record of a sinusoidal wave.

The spectrum only contains one point at 25 Hz with a unit magnitude. Suppose the original time step of 0.05 sec is insufficient to obtain accurate response history results, and a smaller time step of 0.01 sec is used. Using this smaller time step is equivalent to upsampling the original sine wave by a factor of $L = 5$ (see the upsampled data in the upper plot of Figure 2). By performing DFT on the interpolated record, its components in the frequency domain are shown in the lower plot of Figure 2.

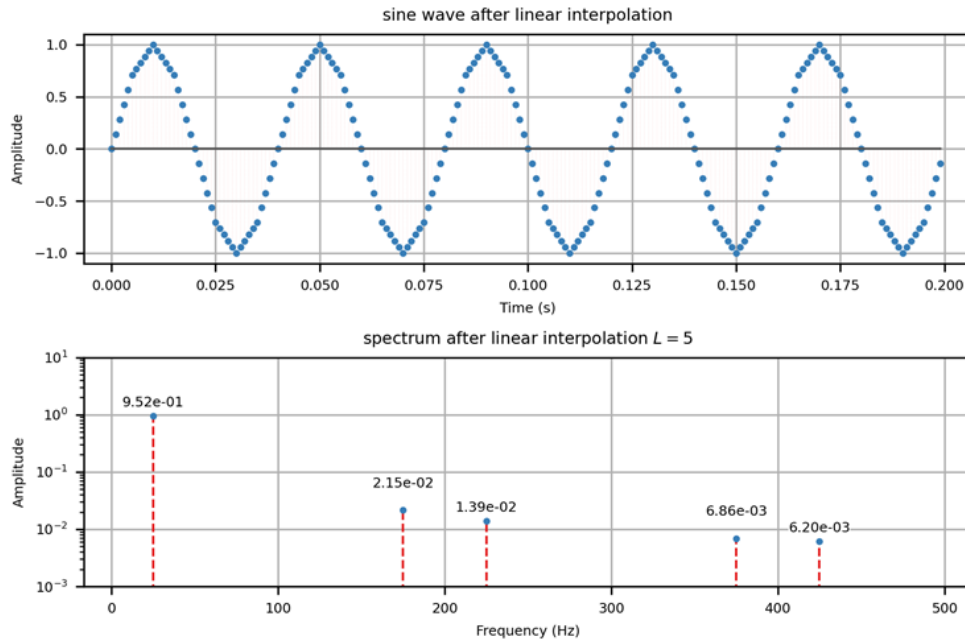


Figure 2. Interpolated sine wave and its components in the frequency domain.

The original component at 25 Hz stays about the same level with a small reduction after interpolation. Additional frequency components are added to the record at 175 Hz, 225 Hz, 375 Hz and 425 Hz. The maximum of those additional components is around 2% (shown as 2.15e-02 in the figure), which appears to be small at first glance. However, noting that there are ω and ω^2 terms in the expressions of the damping force and inertial force. Those additional components would be amplified for the

corresponding frequency, which is 175 Hz. After amplification, its magnitude is comparable to, or sometimes even larger than, that of the original component at 25 Hz. For this specific example, if the response of the transfer function H at 175 Hz is not sufficiently small, the numerical results may contain significant spurious components. This spurious force effect is demonstrated in the following using response history analysis examples.

RESPONSE HISTORY ANALYSIS EXAMPLES

Linear Elastic Example

A simple linear elastic cantilever column of 50 m tall is considered in the response history analysis example. It has a uniform flexural stiffness EI of 200 GPa, and a uniform linear mass density of 1000 kg/m. This column is modelled using five equal-length beam-column elements with a consistent mass matrix. The structural frequencies are 3.17, 19.8, 55.7, 110, 183, 304, 444, 644, 915, and 1346 Hz. The input ground motion is the north-south component of the El Centro earthquake with a sampling time step of 0.02 sec. The Nyquist frequency of the ground motion is 25 Hz. The column is assumed to exhibit 5% damping for all modes. The bell-shaped damping model [8,14-21] is used to simulate this damping with five Type 0 basis functions with its parameters obtained using the method of nonlinear least squares curve-fitting.

The response history analysis is conducted using the Newmark constant acceleration method. Note that this method is selected because it does not introduce algorithmic damping into the system. The spurious effects on the damping forces can be solely related to the viscous damping component without being interfered with algorithmic damping. Three options are considered for the analysis step size and for modifying the input ground motions:

1. Use 0.02 sec as the analysis step size, and keep the original digitized ground motion.
2. Use 0.0025 sec as the analysis step size, and upsample the ground motion with the intermediated data obtained using linear interpolation.
3. Use 0.0025 sec as the analysis step size, and upsample the ground motion with the intermediated data obtained using a filtering process with a Kaiser window. The order and the shape parameter **beta** of the Kaiser window are 160 and 5, respectively. The upsampling process uses the MatLab function **resample** from the signal processing toolbox.

In option 1, the Nyquist frequency of the analysis is 25 Hz. It is only sufficient for obtaining the responses of the first two modes. For options 2 and 3, the new Nyquist frequency is 200 Hz. They are sufficient to cover the first five modes. Note, it is not realistic in practice to have a very small time step to cover all the structural frequencies since most higher modes would not affect the structural responses concerned by most engineers. The first five modes are enough for this cantilever column.

The earthquake ground motions of the three options and their corresponding Fourier spectra are shown in Figure 3. Only the first six seconds of the event, where the motions are large, are used in the analysis and the Fourier spectra computation. The figure shows that all options give very similar ground motions in the time domain with nearly indiscernible differences unless with a close-up view on a smaller time window (see the top right plot of Figure 3). Note the filtering process would generally alter the data at the original time step, but the changes would not be significant. It may also alter the peak ground acceleration. In this case, the peak ground acceleration is increased by about 2%, which is negligible.

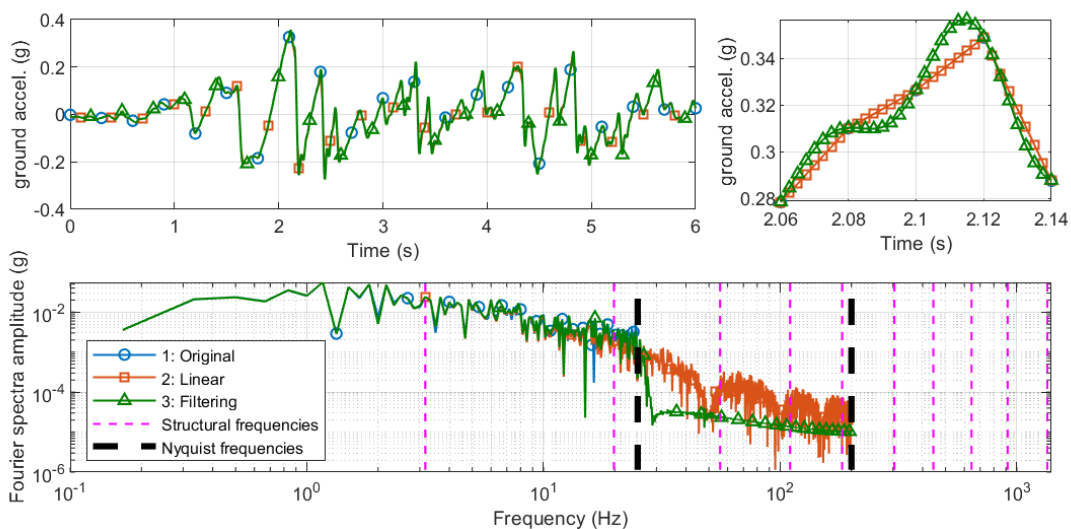


Figure 3. Earthquake ground motions and Fourier spectra using the three options.

In the frequency domain, different options clearly show different spectra for the frequencies between 25 Hz (original Nyquist frequency) and 200 Hz (new Nyquist frequency). Option 2 with linear interpolation has introduced spurious components with frequencies within this range. Option 3 with filtering has managed to reduce the magnitude of these components to a small enough level. Given that the third, fourth, and fifth modes of the structure have frequencies falling within the interval of [25 Hz, 500 Hz], the responses dominated by these three modes are expected to show differences among these options.

Figure 4 shows the column top drift and base shear time histories resulting from the response history analysis using the three options. These two global responses are primarily governed by the lower modes, particularly the first mode. There is almost no major difference between the three options, particularly for options 2 and 3. Option 1 shows noticeable differences due to having a much larger time step. The difference is more obvious for the base shear than the top drift, where the former is more susceptible to the higher modes. This comparison shows that it is important to use an analysis time step that is small enough to sufficiently simulate all the dominant modes, even for the global responses primarily governed by the lower modes.

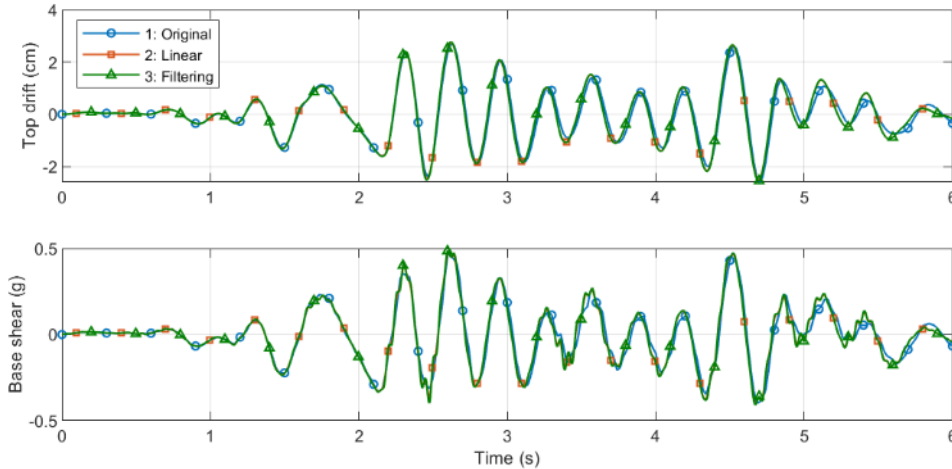


Figure 4. Top drift and base shear time histories using the three options (linear elastic example).

Figure 5 shows the envelopes of the horizontal nodal forces of the three components in the equations of motion: the inertial forces \mathbf{P}_i , the damping forces \mathbf{P}_d , and the constitutive member forces \mathbf{P}_r . The inertial forces \mathbf{P}_i are computed based on the relative accelerations without the contributions from the ground accelerations. The differences among the envelopes using the three options are much more noticeable because these forces are more susceptible to higher modes. Option 1, due to having a larger time step, and option 2, due to having spurious components between the two Nyquist frequencies, fail to yield accurate results for these three forces. Option 3, with spurious components of a smaller magnitude (see Figure 3), would be considered more accurate than the other two. It is also interesting to note that although option 3 has smaller spurious components, it results in larger envelopes for \mathbf{P}_i , \mathbf{P}_d , and \mathbf{P}_r . In this case, the spurious components result in reducing maximum values. Nevertheless, it is yet to be conclusive for general structures and ground motions.

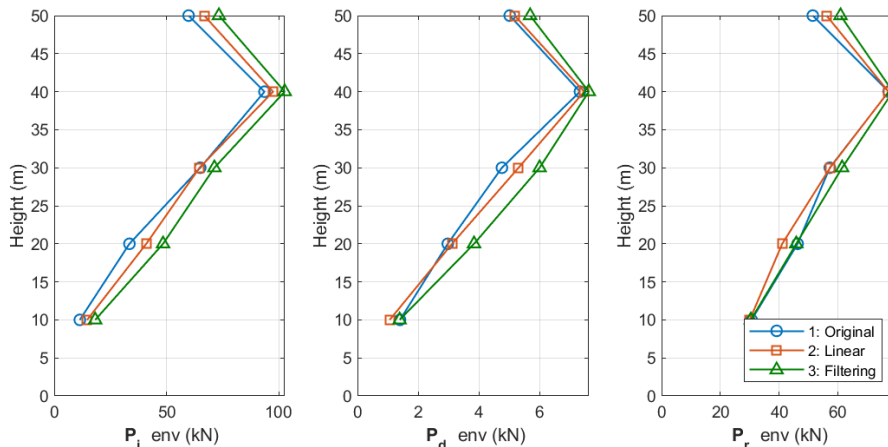


Figure 5. Envelopes of horizontal nodal forces \mathbf{P}_i (inertial forces), \mathbf{P}_d (damping forces) and \mathbf{P}_r (constitutive member forces) using the three options (linear elastic example).

Figure 6 shows the envelopes of the inter-storey shear forces and horizontal nodal accelerations using the three options. The nodal accelerations are the total accelerations with the contributions of the ground accelerations. A similar trend is observed. There are noticeable differences in the envelopes between the options, and option 3 gives the largest envelope. For this case, using linear interpolation for the ground motion has resulted in an unconservative estimate of seismic demands. Using option 3 would be more conservative. It should be noted that horizontal accelerations are crucial for estimating the seismic demands on non-structural components in a multi-storey building. The effects of these spurious forces are particularly important for researchers in the area of non-structural components to take note.

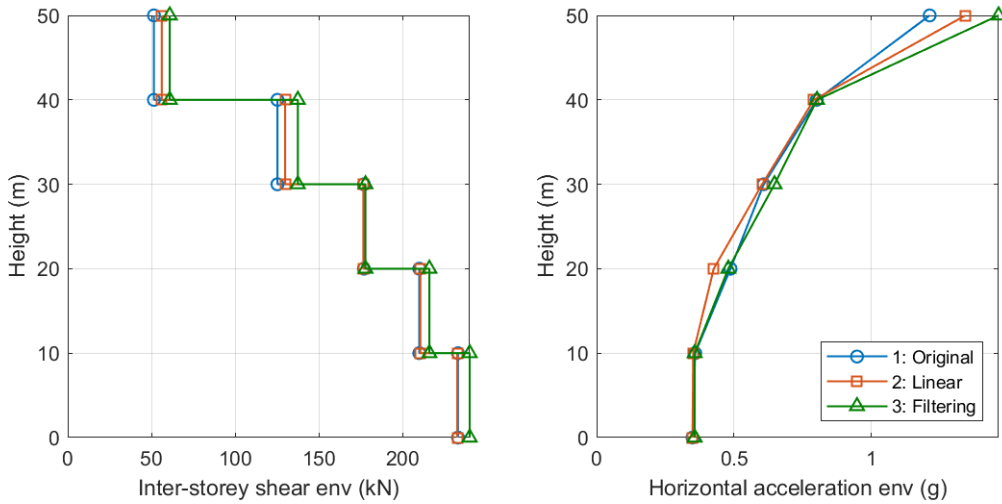


Figure 6. Envelopes of inter-storey shear forces and horizontal nodal accelerations using the three options (linear elastic example).

Nonlinear Inelastic Example

The column used in the previous case is assumed to have the same properties except that it has a yield moment capacity of 2000 kNm with 2% linear kinematic hardening. The same earthquake is applied, but only options 2 and 3 are considered. Option 1 is not considered because it has been proven in the previous example that it would not give sufficiently accurate results due to having a large time step. Due to the capacity in the section moment, yielding at the base would occur during the event.

Figure 7 shows the envelopes of the horizontal nodal forces of the three components, \mathbf{P}_i , \mathbf{P}_d , and \mathbf{P}_r , in the equations of motion. Compared to the previous case, the differences between options 2 and 3, in this case, have become much more prevalent. Option 2, due to having spurious components, results in much smaller nodal forces.

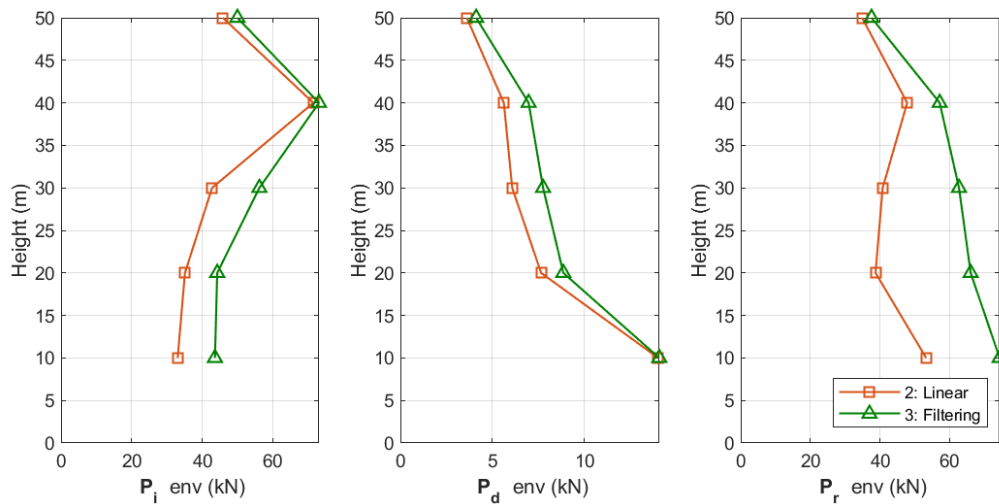


Figure 7. Envelopes of horizontal nodal forces \mathbf{P}_i (inertial forces), \mathbf{P}_d (damping forces) and \mathbf{P}_r (constitutive member forces) using the three options (nonlinear inelastic example).

Figure 8 shows the envelopes of the inter-storey shear forces and horizontal nodal accelerations using the two options. Again, much larger differences between the two options are observed. This example shows that the spurious effects would be significantly amplified in inelastic responses.

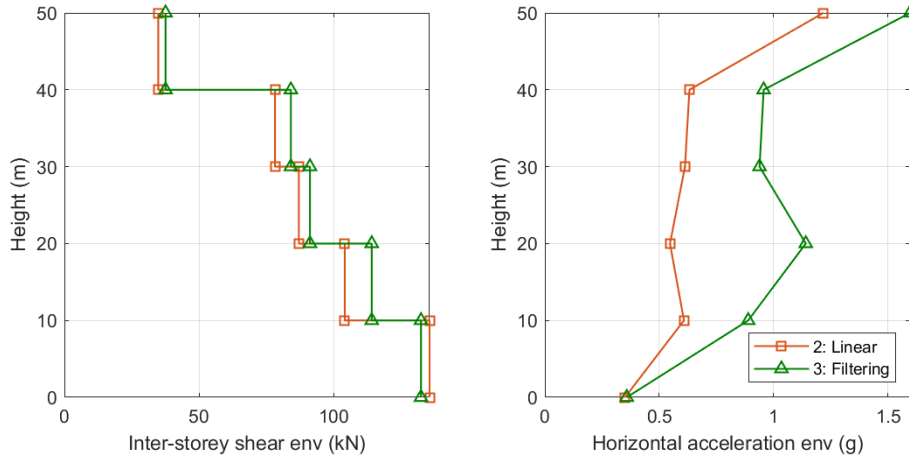


Figure 8. Envelopes of inter-storey shear forces and horizontal nodal accelerations using the three options (nonlinear inelastic example).

RECOMMENDATIONS

It is reasonable to make the following recommendations.

1. To avoid linear interpolation, it is better to have an identical time step size and sampling interval. To this end, analysts shall first choose a proper time step size that would be used in numerical analysis, which is typically smaller than the sampling interval and is determined by the property of the dynamic system of interest. Then, the seismogram shall be processed by upsampling. A low-pass filter with a sufficiently small side lobe level shall be applied to suppress any components above the original Nyquist frequency.
2. The high-frequency noise exists intrinsically and can be spotted analytically. Algorithmic damping can alleviate the issue, but only to a limited degree. Nevertheless, it is still beneficial to adopt a time integration method with adjustable algorithmic damping. In this regard, the de facto Newmark method with constant acceleration, which is widely used, is not recommended.

In terms of numerical analysis of general structures, the following workflow is proposed to improve the reliability of the results generated by numerical analysis.

1. Determine whether the seismograph, in the form of either displacement or acceleration, is properly processed.
2. Determine a proper time step size and, thus, the corresponding upsampling ratio.
3. Design a proper upsampling filter so that the time step size matches the upsampling interval.
4. Develop the structural numerical model with high-frequency modes avoided as much as possible. For example, constraints are better implemented via the Lagrange multiplier method.
5. Perform analysis using filtered records and a time integration method with adjustable algorithmic damping.
6. Examine numerical results to ensure there are no significant high-frequency components.

CONCLUSIONS

One more source of unintended spurious forces in the seismic response history analysis has been discussed, with examples showcasing the spurious force effects on structural responses. This source stems from the linear interpolation of the recorded ground motion data when an analysis time step is chosen to be smaller than the time step used in the data, which is usually needed for better accuracy of responses dominated by higher modes. This linear interpolation would introduce spurious components for frequencies between the original and new Nyquist frequencies, resulting in spurious components in the inertial, damping, and constitutive member forces in the system. As shown in the examples, these spurious forces might result in underestimating seismic demands in some scenarios, and the effects could be much larger in inelastic responses. To avoid these spurious forces, it is recommended to use filtering during the upsampling process to suppress the spurious components in the ground motion input. The examples shown in this paper have demonstrated its success in reducing the spurious force effects. Other recommendations have also been provided, including using a time stepping method with adjustable algorithmic damping.

REFERENCES

- [1] Chrisp, D.J. (1980). *Damping models for inelastic structures*. Master Thesis, Department of Civil Engineering, University of Canterbury, Christchurch, New Zealand.
- [2] Leger, P., and Dussault, S. (1992). “Seismic-energy dissipation in MDOF structures”. *ASCE Journal of Structural Engineering*, 118(5), 1251–1269.
- [3] Bernal, D. (1994). “Viscous damping in inelastic structural response”. *ASCE Journal of Structural Engineering*, 120(4), 1240–1254.
- [4] Carr, A.J. (1997). “Damping models for inelastic analyses.” In *7th Asia-Pacific Vibration Conference*, Kyongju, Korea.
- [5] Hall, J.F. (2006). “Problems encountered from the use (or misuse) of Rayleigh damping”. *Earthquake Engineering & Structural Dynamics*, 35(5), 525–545.
- [6] Charney, F.A. (2008). “Unintended consequences of modeling damping in structures”. *ASCE Journal of Structural Engineering*, 134(4), 581–592.
- [7] Chopra, A.F., and McKenna, F. (2016). “Modeling viscous damping in nonlinear response history analysis of buildings for earthquake excitation”. *Earthquake Engineering & Structural Dynamics*, 45(2), 193–211.
- [8] Lee, C.-L. (2022). “Type 4 bell-shaped proportional damping model and energy dissipation for structures with inelastic and softening response”. *Computers & Structures*, 258, 106663.
- [9] Shing, P.S.B., and Mahin, S.A. (1987). “Elimination of spurious higher-mode response in pseudodynamic tests”. *Earthquake Engineering & Structural Dynamics*, 15(4), 425–445.
- [10] Hulbert, G.M., and Chung, J. (1994). “The unimportance of the spurious root of time integration algorithms for structural dynamics”. *Communications in Numerical Methods in Engineering*, 10(8), 591–597.
- [11] Nyquist, H. (1928). “Certain topics in telegraph transmission theory”. *Transactions of the American Institute of Electrical Engineers*, 47(2), 617–644.
- [12] Dassault Systemes (2017). Abaqus, USA. <http://www.3ds.com/products-services/simulia/products/abaqus>
- [13] McKenna, F., Fenves, G.L., and Scott, M.H. (2000). Open System for Earthquake Engineering Simulation, University of California, Berkeley, USA. <http://opensees.berkeley.edu/>
- [14] Lee, C.-L. (2019). “A novel damping model for earthquake induced structural response simulation.” In *the 2019 Pacific Conference on Earthquake Engineering and Annual NZSEE Conference*, Auckland, New Zealand.
- [15] Lee, C.-L. (2019). “Efficient proportional damping model for simulating seismic response of large-scale structures.” In *Compdyn 2019*, Crete, Greece.
- [16] Lee, C.-L. (2020). “Proportional viscous damping model for matching damping ratios”. *Engineering Structures*, 207, 110178.
- [17] Lee, C.-L. (2020). “Sparse proportional viscous damping model for structures with large number of degrees of freedom”. *Journal of Sound and Vibration*, 478, 115312.
- [18] Lee, C.-L. (2020). “Proportional viscous damping model for matching frequency-dependent damping ratio.” In *7th World Conference in Earthquake Engineering*, Sendai, Japan.
- [19] Lee, C.-L. (2021). “Bell-shaped proportional viscous damping models with adjustable frequency bandwidth”. *Computers & Structures*, 244, 106423.
- [20] Lee, C.-L., and Chang, T.L. (2022). “Numerical evaluation of bell-shaped proportional damping model for softening structures.” In *WCCM-APCOM*, Yokohama, Japan.
- [21] Lee, C.-L., and Chang, T.L. (2023). “Implementation and performance of bell-shaped damping model.” In *Proceedings of the 2022 Eurasian OpenSees Days*, Turin, Italy.